Buckling optimization of blended composite structures using lamination parameters

Xiaoyang Liu, Carol A. Featherston and David Kennedy*

School of Engineering, Cardiff University, Queen's Buildings, The Parade, Cardiff CF24 3AA, UK

* Corresponding author. Email KennedyD@cardiff.ac.uk

Abstract

In this paper, a new lamination parameter based method is proposed for the layup optimization of built-up composite laminates with ply drop-offs. The optimization process is divided into two stages. In the first stage, the multilevel optimization feature of the exact strip software VICONOPT MLO is extended to use the lamination parameters and laminate thicknesses of each component panel as design variables to minimize the weight of the whole structure subject to buckling and lamination parameter constraints. For the second stage, instead of using the common heuristic optimization methods, a novel dummy layerwise branch and bound (DLBB) method is proposed to search the manufacturable stacking sequences to find those needed to achieve a blended structure based on the use of 0°, 90°, +45° and -45° plies and having lamination parameters equivalent to those determined in the first stage. The DLBB method carries out a logical search to circumvent the stochastic search feature of heuristic methods for the determination of stacking sequences. This two-stage method is an extension of a previous highly efficient two-stage method for a single laminate [1]. The effectiveness of the presented method is demonstrated through the optimization of a benchmark wing box.

Keywords: composite; optimization; lamination parameters; blending; branch and bound.

1. Introduction

The optimization of composite laminates has attracted great interest from researchers because of their outstanding mechanical performance and large number of application areas such as aerospace, automotive, marine and civil industries. Composite laminates can be designed to meet different loading conditions by tailoring their stacking sequences, which usually leads to a discrete optimization problem when the ply angles are limited to a set of values (e.g. 0°, 90°, +45° and -45°).

To reduce weight or improve structural performance, the ability to vary the stiffness of laminated composite structures can be used to expand the design space by changing either the fiber orientations or the thicknesses of different laminates in different parts of the structure. In large scale built-up structures, such as an aircraft's wings or fuselage, this results in changes in thickness and lay-up between adjacent panels, potentially leading to stacking sequence mismatches, causing stress concentrations as well as increasing the level of difficulty in the manufacturing process. Therefore, ensuring ply continuity between adjacent panels, which is commonly referred to as the blending problem, is essential [2]. Consequently, the blending constraint together with any layup design constraints (e.g. damage tolerance constraints, disorientation constraints, etc) related to each of the component laminates should be considered when designing multi-panel composite laminated structures in practice.

Genetic algorithms (GAs) have become the most popular method for blending optimization because of their effective performance in discrete processes. Soremekun et al. [3] presented a sublaminate-based method based on GAs for the optimization of a 3×3 array of sandwich panels and an 18-panel horse-shoe structure in which the load for each panel was fixed. Following this, further concepts and methods based on GAs were developed to optimize blended structures. Adams et al. [4–6] proposed the guide-based blending method, in which a template stacking sequence is used as a guide and the blended laminates are then obtained by inwardly or outwardly dropping plies from the guide. Irisarri et al [7] implemented a stacking sequence table (SST) approach with GAs, in which the stacking sequence of a thicker panel is obtained by adding plies to a thinner one, for optimizing blended composite laminates. In Fan et al.'s work [8], a GA which comprises a ply-composition and a ply-ranking chromosome for each individual was proposed for the blending optimization. Yang et al. [8] developed a ply drop sequence method (PDS) which is an extension of the guide-based method. Instead of dropping plies inwardly or outwardly, plies in the thicker panel could be dropped for the thinner panel. In the work of An et al [9], a shared-layer and mutation method (SLM) was proposed to obtain blended laminates. In this method all the layers of the current thinnest laminate are shared with its adjacent laminate, and a mutation operator is used to optimize the non-shared layers. Another popular heuristic algorithm, simulated annealing (SA) was implemented by Zeng et al. with multiple SSTs to obtain blended stacking sequences [11]. A more realistic approach, in which load redistribution within the structure due to changes made during the optimization process is considered, is taken for the case of a wing box by Liu and Haftka [10]. This uses a two-step optimization method, in which the ply orientations to be used are obtained at the first step and the layups for each panel are then obtained considering blending in the second step. Seresta et al. [11] developed a guide-based method with a parallel GA to implement the optimization of the same wing box, obtaining better laminate continuity. A further wing structure was optimized by Jing et al. [12] using the global shear-layer blending method (GSLB), with a blending design scheme using the SST approach also proposed. In their later work [13], the GSLB method was improved by adding a shape prediction algorithm and thickness evaluation technique.

Many effective blending methods have therefore been developed. However, the large number of layers in blended composite structures leads to a large number of design variables, making the optimization inevitably time consuming. As an alternative to these approaches, lamination parameters have been proposed to implement the optimization. This reduces the number of design variables dramatically, since these parameters are independent of the number of plies in the laminate. The stiffness matrix can then be expressed as a linear function of the lamination parameters instead of the conventional set of equations with large numbers of ply orientations. Many optimization techniques [14–23] based on lamination parameters have been developed for a single composite panel. For more complex blended composite structures, IJsselmuiden et al. [24] proposed a multi-step optimization method. In this approach, the thickness and bending lamination parameters of each panel were optimized under a local buckling constraint to minimize the weight during the first step using a successive convex approximation scheme, following which a guide-based method incorporating GAs was conducted to obtain the blended stacking sequences in the second step. In the work of Liu et al. [25], the first order optimization method available in the ANSYS finite element analysis (FEA) software was employed in the first stage to conduct a weight optimization where the bending lamination parameters and the number of plies of each angle were used as design variables. Then in the second stage, the blended stacking sequences of the whole structure were obtained based on the optimized lamination parameters using the shared layer blending (SLB) approach with a permutation GA. Macquart et al. [26] studied the blending constraint in lamination parameters space for the first stage of the optimization, which was then imposed in later works [27–29] where a gradient-based optimizer was employed to optimize lamination parameters and laminate thicknesses, and a guide-based GA was then utilized to search the

corresponding stacking sequences. In the work of Meddaikar et al. [30], a multipoint structural approximation was used in the two-stage optimization, with the mass of a composite structure being minimized by optimizing lamination parameters and laminate thicknesses in the first stage and blended stacking sequences obtained using GAs incorporated with SST in the second stage. Polar parameters can be used as alternatives to the lamination parameters in a two-stage optimization. Although polar parameters make the first stage optimization non-convex, they are true tensor invariants and have direct physical meaning, a characteristic which lamination parameters do not possess. In the work of Panettieri et al [31], a two-stage blending optimization method based on the use of polar parameters was developed. Although GAs are widely used for optimizing blended layups, the drawbacks of implementing a stochastic search and the fact that performance relies heavily on predefined parameters cannot be ignored. Therefore, efforts to develop alternative methods are valuable and continue to be made. Zein et al. [32,33] utilized a constraint satisfaction programming method (CSP) based on enumeration method, during which the number of layers for each ply angle was predefined, in order to optimize blended stacking sequences. Sanz-Corretge [34] developed another CSP method, in which blended laminates are obtained based on a incremental tree technology, adding plies to thinner laminates. A topology inspired method DMTO (Discrete Material and Thickness Optimization) was also developed by Lund in [35,36] for blending optimization. This is different to the other blending methods discussed above, in that it uses gradient-based optimization to obtain blended stacking sequences, avoiding the discreteness of layup design. However, as the blending constraint can be implemented directly and relatively easily in discrete optimization, the development of discrete optimization method is still attractive.

Although the use of FEA in structural optimization provides versatility and is widely used, the computational cost is high. The highly efficient panel analysis and optimum design software, VICONOPT [37,38] which also includes lamination parameters as design variables [39] performs buckling analyses based on the exact strip method and the Wittrick-Williams algorithm [40,41] and provides a potential alternative. However, it is restricted to applications involving prismatic structures which precludes the optimization of more complex three-dimensional structures, To address this a multilevel optimization framework VICONOPT MLO [3,4] has been developed, in which a static FEA analysis is conducted for the whole structure to obtain load distributions, after which VICONOPT is used to optimize the constituent prismatic panels, combining the benefits of the two different types of methods whilst avoiding the drawbacks of each.

The authors' previous work [1] implemented a two-stage layup optimization for a single laminate in which VICONOPT was employed to optimize the lamination parameters and laminate thicknesses in the first stage, and then a highly efficient layerwise branch and bound method (LBB) which implements a logic-based search was used to obtain the manufacturable stacking sequences corresponding to these optimized lamination parameters in the second stage. In the present study, this two-stage optimization is extended to blended composite structures. This is achieved by extending VICONOPT MLO to use lamination parameters and laminate thickness as design variables instead of the layup itself and employing it in the first stage of the optimization. For the second stage, the logic based LBB is extended to the blending problem, for which a novel dummy layerwise branch and bound method (DLBB) is proposed and utilized to search the blended layups for the whole structure. The proposed method is applied to a wing box benchmark [42] to demonstrate its efficacy and potential.

Section 2 of this paper outlines the basic procedures for the two-stage optimization. Section 3 describes the proposed two-stage method for blended laminates, Section 4 presents numerical results for the benchmark wing box, and brief conclusions are given in Section 5.

2. Outline of optimization procedure

2.1 Optimization features of VICONOPT and VICONOPT MLO

The exact strip software VICONOPT, which comprises the earlier programs VIPASA (Vibration and Instability of Plate Assemblies including Shear and Anisotropy) [44] and VICON (VIPASA with CONstraints) [45], performs buckling, postbuckling and free vibration analyses based on the Wittrick-Williams algorithm. The major advantage of the exact strip method over FEA is its high efficiency, with VIPASA and VICON shown to be 1000 and 150 times faster than FEA for buckling analysis, respectively [37]. In continuous optimization problems, the method of feasible directions [46] is combined with a thickness factoring approach [37] to obtain just stable results during the iterative optimization process. Buckling constraints are evaluated by the highly efficient exact strip method with the corresponding sensitivities obtained using an accelerated finite difference technique [37]. Local linear approximations are applied to buckling constraints during the gradient-based optimization.

VICONOPT MLO [42,43] is a software package providing a multilevel optimization framework based on the optimization features of VICONOPT for each component panel and FEA for the whole structure. A static analysis of the whole structure (system) is first performed by FEA. Then, optimization models are created for each component panel based on the results from the FEA (stress distribution, geometry, etc.) and a set of user-defined design variables. After these panels are optimized, the designs are incorporated into the system level finite element model and a new static analysis is performed to determine the updated load distributions. These newly obtained load distributions are then used at the panel level to re-optimize the component panels. This process is repeated until there is convergence of the total mass, as well as the individual mass and stress distribution for each panel. The optimum solution is thus reached in an efficient manner, shown to be around 4 times faster than the same optimization based purely on FEA [42].

2.2 Two stage optimization method for single laminate

The authors' two-stage method for layup optimization of a single laminate with consideration of practical layup design constraints using lamination parameters is given in [1]. Since the method proposed in this paper is an extension of the method for a single laminate, the parts which are also necessary for the new method will be repeated here.

According to [47], four major layup design constraints need to be taken into account for composite laminate design.

(1) Contiguity constraint: the maximum number of successive plies with the same orientation is limited to an integer n_{cont} to minimize edge splitting. $n_{\text{cont}} = 4$ in this paper.
(2) Disorientation constraint: the difference between two adjacent plies should be no greater than an angle θ_{diff}. This constraint is applied to avoid microcracking. $\theta_{\text{diff}} = 45°$ in this paper.
(3) Minimum percentage constraint: each fiber orientation should comprise a proportion of at least p_m of the total layup to prevent the matrix from being exposed to direct loads and provide sufficient damage tolerance to the laminate. $p_m = 10\%$ in this paper.
(4) Damage tolerance constraint: putting 0° and 90° plies on the exterior surfaces of the laminate should be avoided to provide sufficient damage tolerance after impact.

These four layup design constraints are all included in the second stage of the optimization using the logic-based method and constraint (3) is also imposed in the first stage of the optimization.

2.2.1 First stage optimization for single laminate

2.2.1.1 Lamination parameters

According to classical laminate theory [48], the stress-strain relationship for a composite laminate can be described by

$$\begin{bmatrix}\mathbf{N}\\ \mathbf{M}\end{bmatrix}=\begin{bmatrix}\mathbf{A} & \mathbf{B}\\ \mathbf{B} & \mathbf{D}\end{bmatrix}\begin{bmatrix}\boldsymbol{\varepsilon}^{0}\\ \boldsymbol{\kappa}\end{bmatrix} \tag{1}$$

where **N** and **M** are vectors of in-plane forces and moments per unit width, **A**, **B** and **D** are membrane, coupling and bending stiffness matrices, $\boldsymbol{\varepsilon}^{0}$ is a vector of in-plane strains and $\boldsymbol{\kappa}$ is a vector of mid plane curvatures.

For symmetric laminates, the coupling matrix **B** is null and will be ignored in this paper for simplicity. The membrane and bending stiffness matrices **A** and **D** can be expressed in terms of 8 lamination parameters ξ_j^k (j=1,2,3,4; k=*A, D*) [49] and material stiffness invariants **U**:

$$\begin{bmatrix}A_{11}\\ A_{22}\\ A_{12}\\ A_{66}\\ A_{16}\\ A_{26}\end{bmatrix}=h\begin{bmatrix}1 & \xi_1^A & \xi_2^A & 0 & 0\\ 1 & -\xi_1^A & \xi_2^A & 0 & 0\\ 0 & 0 & -\xi_2^A & 1 & 0\\ 0 & 0 & -\xi_2^A & 0 & 1\\ 0 & \xi_3^A/2 & \xi_4^A & 0 & 0\\ 0 & \xi_3^A/2 & -\xi_4^A & 0 & 0\end{bmatrix}\begin{bmatrix}U_1\\ U_2\\ U_3\\ U_4\\ U_5\end{bmatrix} \tag{2}$$

$$\begin{bmatrix}D_{11}\\ D_{22}\\ D_{12}\\ D_{66}\\ D_{16}\\ D_{26}\end{bmatrix}=\frac{h^3}{12}\begin{bmatrix}1 & \xi_1^D & \xi_2^D & 0 & 0\\ 1 & -\xi_1^D & \xi_2^D & 0 & 0\\ 0 & 0 & -\xi_2^D & 1 & 0\\ 0 & 0 & -\xi_2^D & 0 & 1\\ 0 & \xi_3^D/2 & \xi_4^D & 0 & 0\\ 0 & \xi_3^D/2 & -\xi_4^D & 0 & 0\end{bmatrix}\begin{bmatrix}U_1\\ U_2\\ U_3\\ U_4\\ U_5\end{bmatrix} \tag{3}$$

where the material stiffness invariants **U** and stiffness properties **Q** are:

$$\begin{bmatrix}U_1\\ U_2\\ U_3\\ U_4\\ U_5\end{bmatrix}=\frac{1}{8}\begin{bmatrix}3 & 3 & 2 & 4\\ 4 & -4 & 0 & 0\\ 1 & 1 & -2 & -4\\ 1 & 1 & 6 & -4\\ 1 & 1 & -2 & 4\end{bmatrix}\begin{bmatrix}Q_{11}\\ Q_{22}\\ Q_{12}\\ Q_{66}\end{bmatrix} \tag{4}$$

$$\begin{cases}Q_{11}=E_{11}{}^2/(E_{11}-E_{22}\upsilon_{12}{}^2)\\ Q_{22}=E_{11}E_{22}/(E_{11}-E_{22}\upsilon_{12}{}^2)\\ Q_{12}=\upsilon_{12}Q_{22}\\ Q_{66}=G_{12}\end{cases} \tag{5}$$

E_{11} is the longitudinal Young's modulus, E_{22} is the transverse Young's modulus, G_{12} is the shear modulus, v_{12} is the major Poisson's ratio and h is the thickness of the laminate.

The lamination parameters are obtained by the following integrals

$$\begin{bmatrix}\xi_1^k\\ \xi_2^k\\ \xi_3^k\\ \xi_4^k\end{bmatrix}=\int_{-h/2}^{h/2} Z^k \begin{bmatrix}\cos 2\theta\\ \cos 4\theta\\ \sin 2\theta\\ \sin 4\theta\end{bmatrix} dz, k=A,D, \begin{cases} Z^A = 1/h \\ Z^D = 12z^2/h^3 \end{cases} \tag{6}$$

where θ represents the ply angle at depth z below the mid-surface. $\xi_3^A$is zero for a balanced laminate and $\xi_4^{A,D}$ are zero if the ply angles are limited to 0°, 90°, +45° and -45°.

2.2.1.2 Optimization for lamination parameters

Lamination parameters have been introduced as design variables in VICONOPT [39], expanding the design space and reducing the number of design variables. During the first stage, lamination parameters and laminate thickness are optimized using the optimization features of VICONOPT subject to buckling and lamination parameter constraints. Each of the lamination parameters ξ_j^k lies between -1 and 1, and they are further restricted by 25 constraints [39,50] as follows.

$$2\left|\xi_1^k\right| - \xi_2^k - 1 \le 0, \;\; 2\left|\xi_3^k\right| + \xi_2^k - 1 \le 0, \quad k = A, D \tag{7}$$

$$2\left|\xi_1^B\right| + \xi_2^B - 2 \le 0, \quad 2\left|\xi_3^B\right| + \xi_2^B - 2 \le 0, \qquad \left|\xi_1^B\right| + \left|\xi_3^B\right| - 1 \le 0 \tag{8}$$

$$4\left(\xi_i^D + r\right)\left(\xi_i^A + r\right) \ge \left(\xi_i^A + r\right)^4 + 3\left(\xi_i^B\right)^2, \;\; i = 1,2,3, \;\; r = \pm 1 \tag{9}$$

$$16(2\xi_1^D + r\xi_2^D + rs)\left(2\xi_1^A + r\xi_2^A + rs\right) \ge \left(2\xi_1^A + r\xi_2^A + rs\right)^4 + 12(2\xi_1^B + r\xi_2^B)^2, \quad r = \pm 1, s = 1, -3 \tag{10}$$

$$16(2\xi_3^D + r\xi_2^D + rs)\left(2\xi_3^A + r\xi_2^A + rs\right) \ge \left(2\xi_3^A + r\xi_2^A + rs\right)^4 + 12(2\xi_3^B + r\xi_2^B)^2, \quad r = \pm 1, s = 1, -3 \tag{11}$$

$$4(\xi_1^D + r\xi_3^D + s)\left(\xi_1^A + r\xi_3^A + s\right) \ge \left(\xi_1^A + r\xi_3^A + s\right)^4 + 3(\xi_1^B + r\xi_3^B)^2, \quad r = \pm 1, \;\; s = \pm 1 \tag{12}$$

If the percentage of plies at each ply orientation level is required to be below a minimum value p_m, the feasible regions are further restricted as follows [1] :

$$2\left|\xi_1^A\right| - \xi_2^A + 4p_m - 1 \le 0, \;\; 2\left|\xi_3^A\right| + \xi_2^A + 4p_m - 1 \le 0 \tag{13}$$

$$2\left|\xi_1^D\right| - \xi_2^D + 16{p_m}^3 - 1 \le 0, \;\; 2\left|\xi_3^D\right| + \xi_2^D + 16{p_m}^3 - 1 \le 0 \tag{14}$$

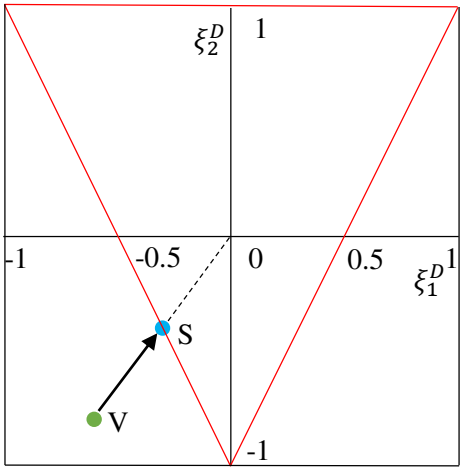

Fig. 1. An example for the illustration of penalty method on feasible region $\xi_{1,2}^D$ (the original point V which is outside the feasible region is moved to the just feasible point S).

These constraints which define feasible regions of the design space are essential for lamination parameter optimization. Violation of these constraints means the lamination parameter values cannot be achieved using the selected predefined ply angles [51]. The method of feasible directions with buckling constraints imposed by linear approximations based on the buckling load factors obtained using exact strip analysis is used to optimize the design variables. These non-linear lamination parameter constraints are imposed using a penalty function method [39]. For cases where the lamination parameter constraints are violated, all lamination parameters ξ_j^k $(j = 1,2,3; k = A, B, D)$ are multiplied by a scalar α $(0 < \alpha < 1)$ which is determined by a bisection method, in order to move the outlying lamination parameters to the boundary of the feasible region, making the most critical constraint just satisfied. An example is shown in Fig.1, where it can be seen that point V is outside the feasible region of $\xi_{1,2}^D$ and violates the constraint (7), so the penalty function forces it to point S where the constraint is just satisfied.

As well as the penalized lamination parameters $\alpha\xi_j^k$ $(j = 1,2,3; k = A, B, D)$, the laminate thickness h is also replaced by αh in the stiffness calculation, so that infeasible configurations tend to violate the buckling constraints and hence appear unattractive to the optimizer. However, the laminate thickness h is not penalized in the mass calculation, to ensure that the infeasible configuration will not have an artificially attractive objective function.

2.2.2 Second stage optimization for single laminate

A logic-based layerwise branch and bound method which combines a global layerwise technique with the branch and bound method was used to search the stacking sequences in order to match the optimized lamination parameters obtained in the first stage [1]. The decision tree of the branch and bound method is comprised of several levels of branches (i.e. choice options). The objective function Γ is obtained by calculating the difference between the target lamination parameters and the actual lamination parameters of the real layup. In order to choose a branch which is close to the target lamination parameters, the branching process predicts the route to proceed with in the next level of the decision tree by considering bounds on the achievable Γ. The upper bound takes the value of the incumbent best solution, and the lower bound of each branch is calculated by subtracting the maximum achievable

contribution of the remaining levels from the exact value of Γ obtained from the contributions of the preceding levels. In this way, branches whose lower bounds are higher than the current upper bound or which violate the layup design constraints can be discarded directly. A detailed example to illustrate this process can be found in [1]. Once the branching process reaches the bottom of the decision tree or the current branch cannot improve on Γ regardless of which lower branches are chosen, the backtracking process starts to subsequently check the remaining possibilities in the decision tree to avoid missing the best result. The branch and bound process performs most efficiently on small problems or when there is a good incumbent solution.

Therefore, a global layerwise technique is incorporated with the branch and bound method to improve the searching efficiency. Ply angles are optimized successively from the outer plies of the laminate. Initially only two plies are optimized at once. When there is no further improvement in Γ, the optimization considers four plies at once, and so on until in the final cycle all the plies are optimized within one decision tree. The benefit of this approach is that the branch and bound method initially searches layups with small decision trees, meaning good incumbent solutions can be obtained quickly in the early stages. Afterwards, when searching layups with larger decision trees, the previous incumbent solution is used in the bounding process, enabling many branches to be pruned away without being searched. In this way, large reductions in solution time can be achieved using the global layerwise technique.

3. Optimization procedure for blended laminates

In this section, the two-stage layup optimization method presented in Section 2 is extended for the optimization of blended laminates. Instead of using VICONOPT, the first stage optimization uses VICONOPT MLO, which is improved in this paper by introducing lamination parameters as design variables. In the second stage, in order to impose the blending constraint in the logic-based method, a dummy layerwise branch and bound method is proposed to search the stacking sequences to match the target lamination parameters obtained in the first stage.

3.1 First stage optimization for blended laminate

The multilevel optimization features of VICONOPT MLO were introduced in Section 2.1. In its previous format, the stacking sequence of each panel was fixed during the optimization, the thickness of each layer was optimized continuously and no allowance was made for practical laminate design rules and layup design constraints. In this work, VICONOPT MLO is modified to perform layup optimization of blended composite structures and to obtain more manufacturable designs based on the use of lamination parameters as design variables. This new version of the software combines optimizing the lamination parameters for each component panel in VICONOPT using the new capability described in Section 2.2.1.2 with static FEA of the whole structure using ABAQUS [52] to obtain load distributions, using stiffness matrices created based on lamination parameters and laminate thicknesses rather than specific layups. During the first stage, the optimized lamination parameters and laminate thicknesses of each component panel are determined. These are then used to obtain stacking sequences in the second stage.

3.2 Second stage optimization for blended laminate

In the second stage of the optimization process, a dummy layerwise branch and bound (DLBB) method illustrated in Fig. 2 is developed to search the stacking sequences for the whole structure. The optimized

lamination parameters obtained in the first stage are used as the target values for the DLBB which optimizes the stacking sequences to match these target values as closely as possible. Note that this second stage DLBB optimization can be used with VICONOPT MLO as well as any other optimizers which are able to optimize lamination parameters in the first stage optimization. Instead of searching the stacking sequence stochastically as in a heuristic algorithm, the dummy layerwise technique and the branch and bound method make DLBB a logical search based method. In this work blending and four layup design constraints are implemented through the DLBB.

Once the first stage of the optimization is completed, the corresponding number of plies in each panel is determined and fixed. Before optimizing the stacking sequences in the second stage, all panels are ranked in terms of their number of plies. Then for each panel except the thickest one, dummy plies are added on top to give all panels the same number of plies as the thickest one, forming a dummy layerwise table as shown in Fig. 3. The aim of the DLBB is to minimize the objective function Γ obtained by calculating the difference between the target lamination parameters and the actual lamination parameters related to the chosen ply orientations as follows

$$\Gamma = \sum_{k=1}^{n} \Gamma_{panel\ k} \tag{15}$$

$$\Gamma_{panel\ k} = \sum_{i=1}^{3} \sum_{j=A,D} w_j \left| \xi^{j}_{i(k)(actual)} - \xi^{j}_{i(k)(target)} \right| \tag{16}$$

where n is the number of panels, $w_{A,D}$ are weighting factors, $\xi^{A,D}_{1,2,3(k)(target)}$ are the target lamination parameters for panel k, and $\xi^{A,D}_{1,2,3(k)(actual)}$ are the actual lamination parameters of the chosen layup of panel k.

As in LBB [1], the current best result is used as the upper bound in the branch and bound method, and the lower bound is obtained by subtracting the maximum achievable contribution of the remaining levels in the decision tree from the exact value of Γ obtained by only considering the contributions of the chosen levels. Based on these bounds, the branching process selects the branches for the next level with the aim of minimizing the value of Γ.

In this case however, dummy plies which are used to impose the blending constraint are added into the layerwise process. Since these dummy layers do not contribute to the stiffness of the laminate, they are not included in the branch and bound search. As illustrated in Figs. 2 and 3, the dummy layerwise technique consists of three loops: the cycle, pass, and case, which optimize the ply orientations successively, working inwards from the outer plies which make the most important contributions to the flexural lamination parameters $\xi^{D}_{1,2,3}$. As shown in Fig. 3 for a symmetric layup, only two plies from each panel are optimized at once in the first cycle using the branch and bound method, then three, and so on until in the final cycle all the plies are optimized together. As the branch and bound process starts with small problems which only considers a few plies, good results can be obtained quickly, which are then used as upper bounds when searching the increasingly larger number of plies in subsequent cycles, and hence many branches can be discarded without being explored, reducing the searching time.

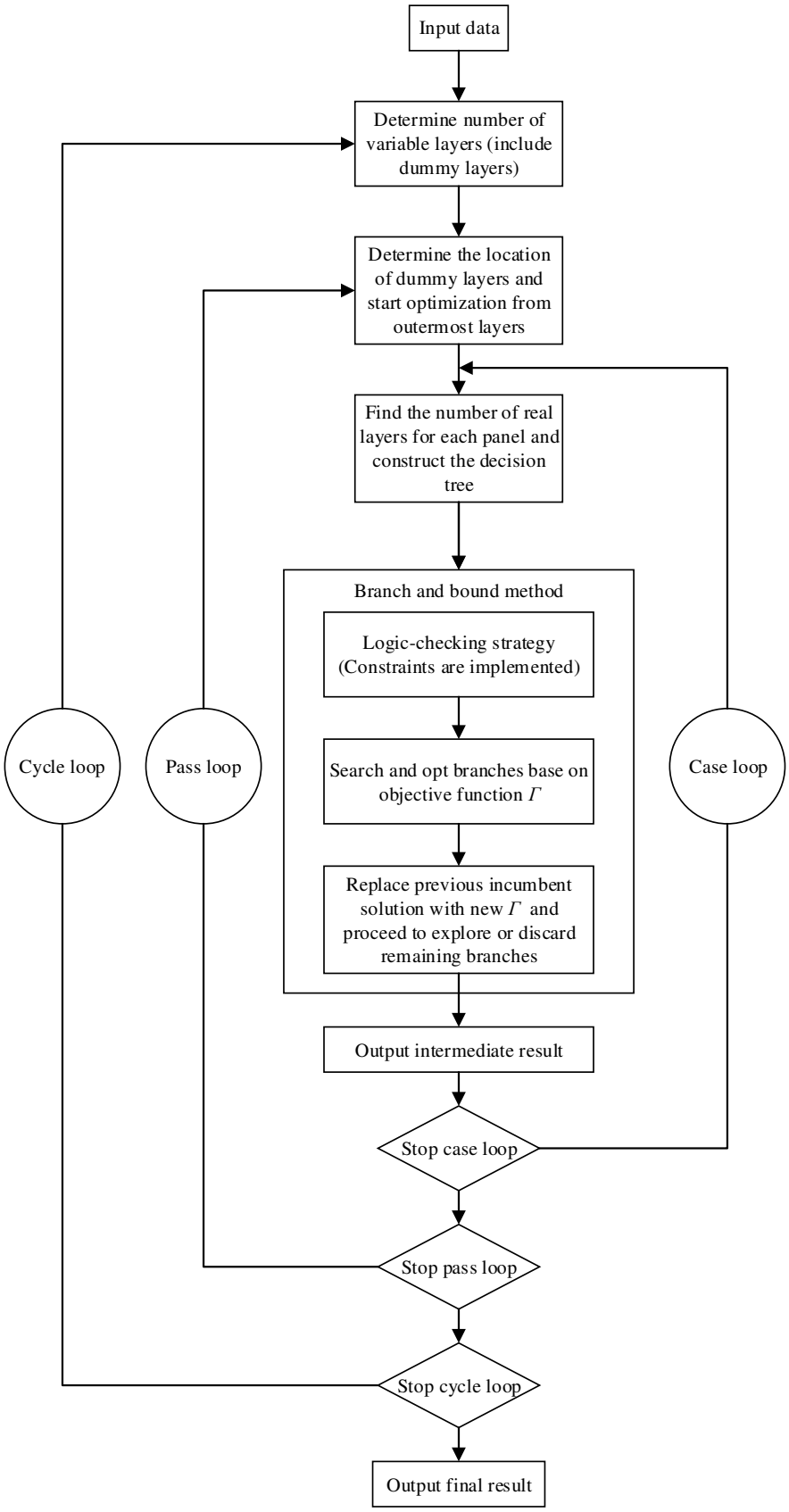

Fig. 2. Flowchart of the dummy layerwise branch and bound (DLBB) method.

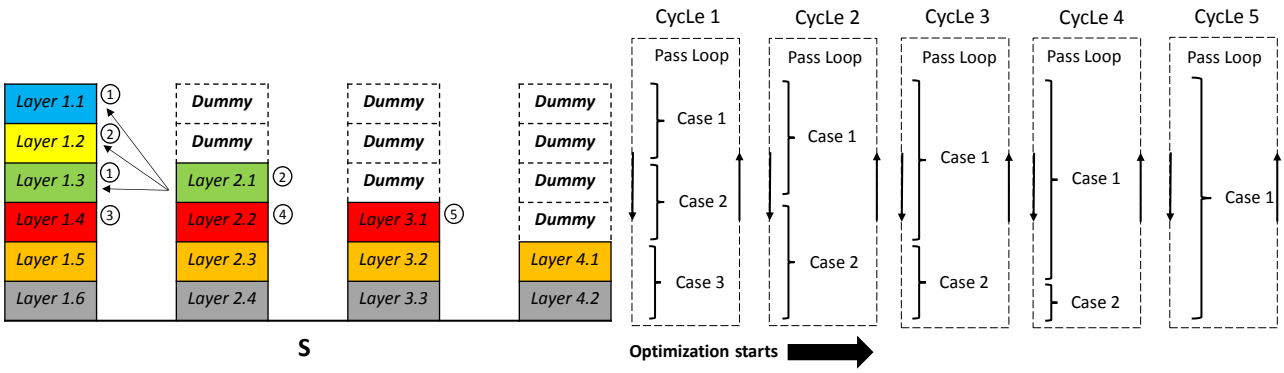

Fig. 3. The dummy layerwise technique: starting layout of the dummy layerwise table.

The blending process of the DLBB method is illustrated in Figs. 3-6 with the example of a blended structure comprising four panels whose symmetric layups contain 12, 8, 6 and 4 layers, respectively. As can been seen from Fig. 3, in the first case of the first cycle, only the two outer real layers in the thickest panel are optimized. A decision tree for a possible layup resulting from the branch and bound method is shown in Fig 4 (a). In order to impose the blending constraint, the order of layers for the branch and bound optimization in a case can be described by:

$P_{i.j}$
$i = 1, j = m \times n - m + n$ for the first layer
$i = i + 1$ if the layer to the right is not a dummy layer
$i = 1, j = j + 1$ if the layer to the right is a dummy layer or $i > i_{max}$

where P_{ij} is the position of the layer in the dummy layerwise table, i and j represent the column number and row number in the dummy layerwise table respectively, m and n are the cycle number and case number respectively, and i_{max} is equal to the total number of panels. In Fig. 3, the order of the layers to be optimized in the first and second cases of the first cycle are shown in circles. In the first case, the position of the first layer to be optimized in the dummy layerwise table is $P_{1.1}$. As the layer to the right is a dummy layer, the position of the next layer is $P_{1.2}$. Similarly, for the second case, the positions of the layers to be successively optimized are determined as $P_{1.3}$, $P_{2.3}$, $P_{1.4}$, $P_{2.4}$, $P_{3.4}$, based on which the blended layups can be obtained in the branch and bound search as described in the following paragraph.

In the second case of the first cycle, the newly optimized layup of the first case is used as the starting layup. The corresponding decision tree for a possible layup, in which the branches at different levels are for different panels is shown in Fig. 4 (b). As can been seen from Fig. 3, the optimization starts from layer 1.3, then goes to layer 2.1 (note that the position of layer 2.1 in the table is $P_{2.3}$). Since layers 1.1, 1.2 and 1.3 have already been chosen, layer 2.1 can be chosen to match any of these. After that, layers 1.4, 2.2 and 3.1 are selected. For layer 2.2, the choices available are the angles of the layers which are below the layer in the panel to its left that layer 2.1 has just been chosen to match. The rest of the choices for layer 2.2 in the decision tree are pruned directly by the bounding process. In addition, according to the chosen layup of the panel at the current level, the checking strategy developed in [1] is implemented to determine which ply is to be pruned to satisfy the layup design constraints applied for a single panel. In the same way, for layer 3.1 there are two choices, namely to match layer 2.1 or layer 2.2. Moreover, after layer 3.1 has been chosen, the branch and bound method will go back to check the rest of the possibilities remaining in the decision tree to avoid missing the best layup for the layers in the current

case. As a lower value of Γ has been obtained in the current case, more branches in the rest of the tree can be pruned directly during this backtracking procedure. A benefit of the backtracking procedure and optimization order described above is that decisions regarding intermediate results are made based on a balance between all the panels for each case loop.

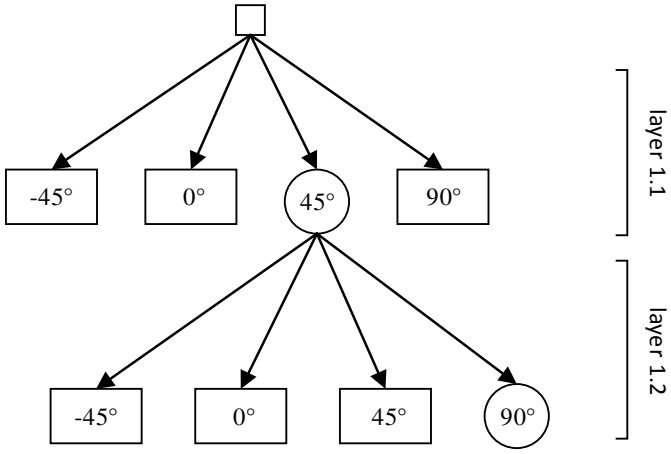

(a)

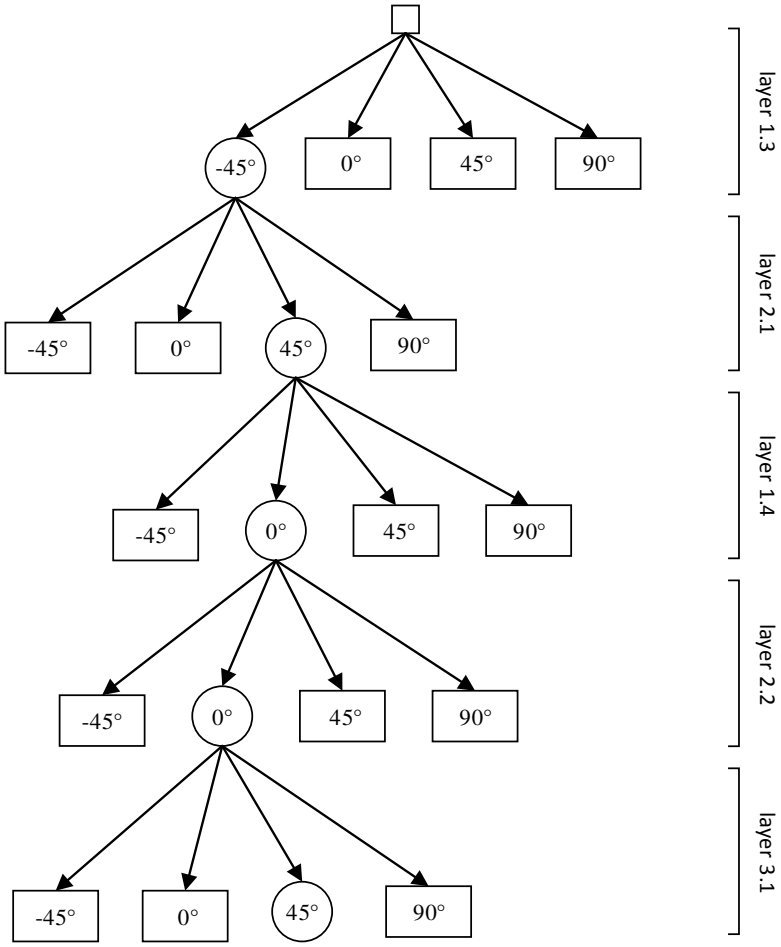

(b)

Fig. 4. Decision trees with a possible determined layup: (a) in the first case of the first pass of the first cycle; (b) in the second case of the first pass of the first cycle.

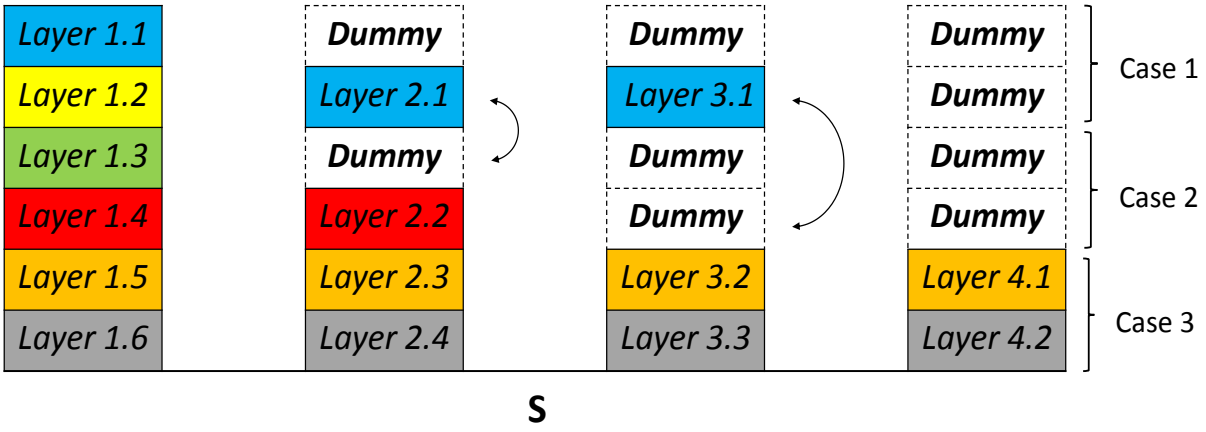

Fig. 5. Layout changes after the first pass of the first cycle.

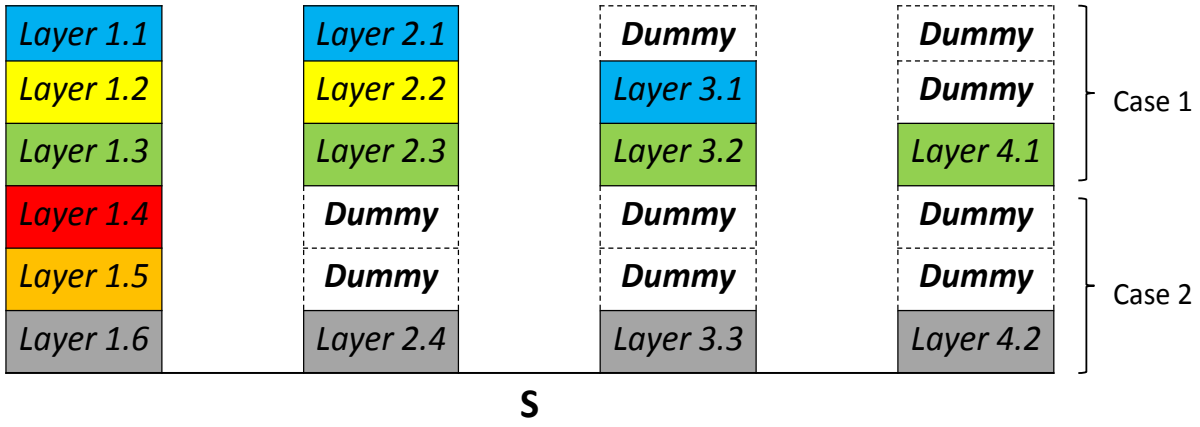

Fig. 6. A possible starting layup for the second cycle.

The positions of the dummy layers in the dummy layerwise table are changed according to the layer choices after each case, enabling flexibility in determining the layer drop-off location. Once a layer has been chosen to match the layer which is located in the panel to the left in the former case, the layer in the current case will be dropped and moved up to the corresponding former case, and a dummy layer in the former case will be swapped to the current case. For example, if layers 2.1, 2.2 and 3.1 are chosen to match layers 1.2, 1.4 and 2.1, respectively, the dummy layers in the first case swap with the real layers in the second case as shown in Fig. 5. Hence, the layout of the dummy layerwise table and the optimized order of the layers are changed for the next pass. In the next pass loop, the layer moved up will be optimized in the same case with the layer it is chosen to match, so as to ensure the blending constraint is satisfied. Furthermore, after the dummy layers are swapped to the new case, they will be located from the top to the bottom in each case to provide more choices for the real layers.

After the last case loop in a pass loop is completed, a new pass loop starts and repeats the process based on the newly obtained layup from the last loop until convergence to a constant Γ is achieved. This current best result is then used as the starting layup for the next cycle loop where a larger number of layers can be optimized in a case loop. Fig. 6 shows a possible starting layout for the dummy layerwise table for the second cycle. As the new case contains the layers from the two cases in previous cycle, the dummy layers in each new case are relocated from the top to the bottom at the beginning of the new cycle. As can be seen in Fig. 6, the positions of the real layers are more flexible in these cases of the

second cycle because more layers are allowed to be optimized together. Based on the process described above, the blended layup can be obtained logically by the branch and bound method embedded within the dummy layerwise technique. To generate the initial layup for the second stage optimization, the method described in [1] is used to create the layup for the thinnest panel. A multiple of a ply group of the four angles such as $[-45/0/45/90]_S$, which can be used for laminates with numbers of plies equal to multiples of eight is first generated. For panels with other numbers of plies, combinations of the following three groups $[-45/45]_S$, $[90 \text{ or } 0]_S$, [0] are added, adjacent to plies with the same orientation to avoid violating the disorientation constraint. Following this, the thicker laminates are successively obtained by adding combinations of the groups described above to ensure the blending constraints as well as other layup design rules are satisfied. Hence, the DLBB method starts with a blended layup which satisfies all the constraints, ensuring that all intermediate results and the final result satisfy these constraints.

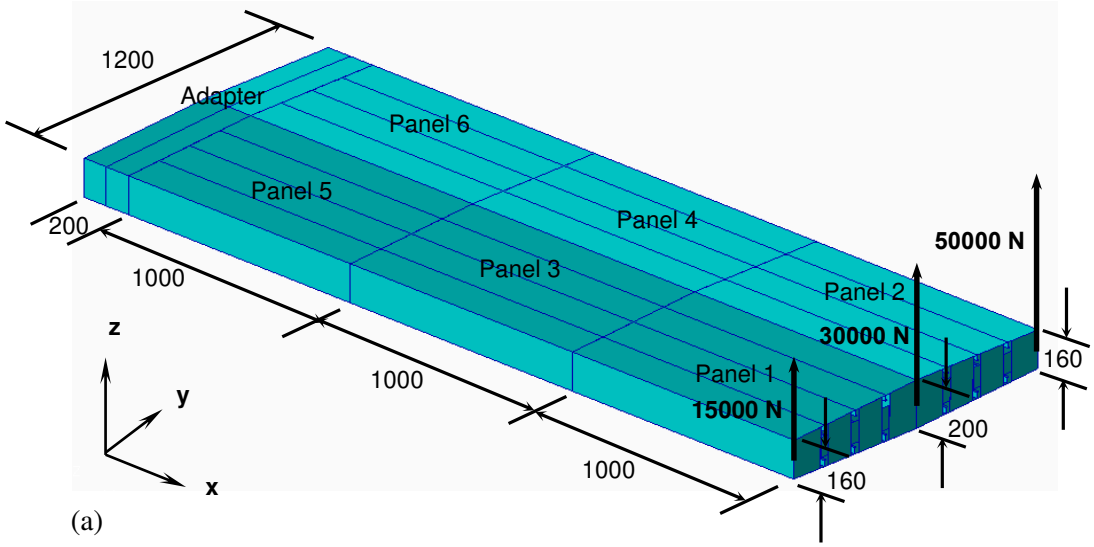

(a)

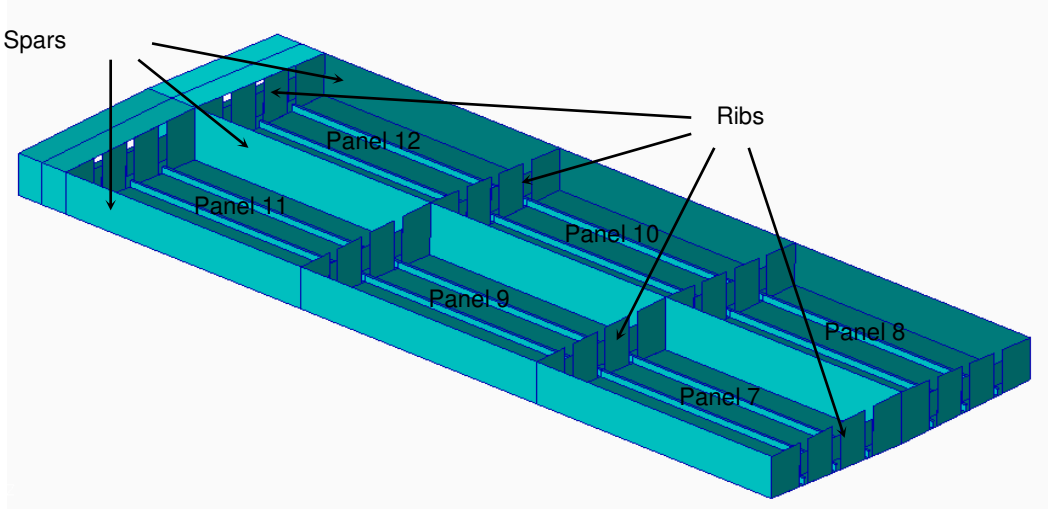

(b)

Fig. 7. (a) Geometry of the wing box and the load case (dimensions in mm). (b) Bottom panels, ribs and spars.

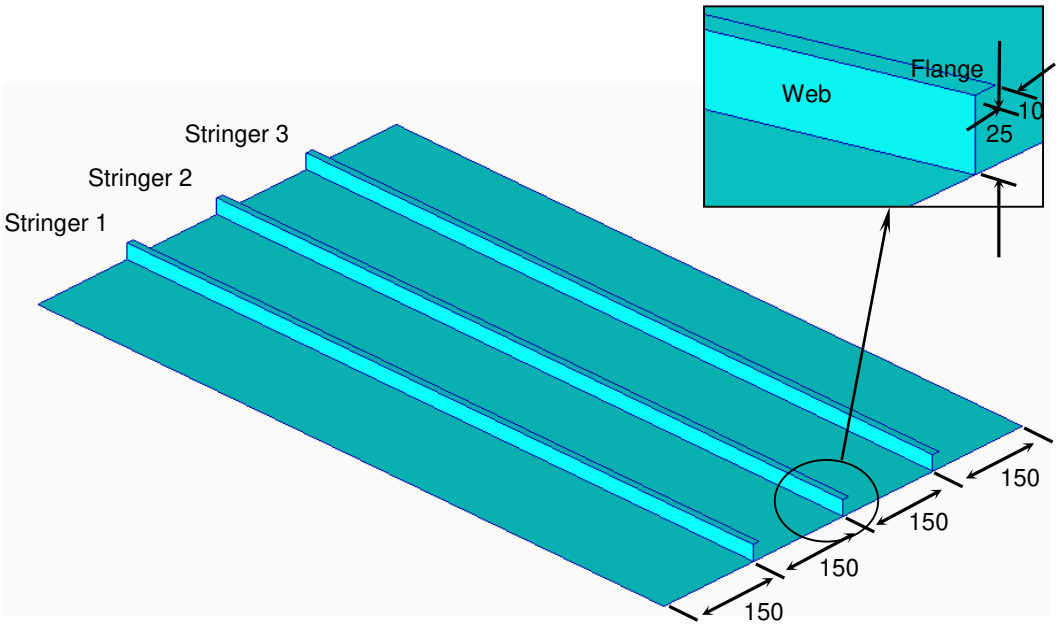

Fig. 8. Geometry of the component panels (dimensions in mm).

4. Results

The benchmark wing box structure used in previous work on VICONOPT MLO [42] is presented in this paper to validate the proposed two-stage method. As shown in Fig. 7, the wing comprises six panels on the top, six panels on the bottom, four ribs and three spars. The details of the skin panels are shown in Fig. 8. Each panel has three L-shaped stringers reinforcing longitudinal stiffness and increasing local buckling capability. All the components are assumed to be rectangular with uniform thickness, and are rigidly attached to each other. The wing is made of high strength carbon-epoxy and the material properties are given in Table 1. Three concentrated loads of magnitudes 50000 N, 30000 N and 15000 N are applied at the rib at the free end, inducing upward bending and twisting of the wing. To model realistic boundary conditions, the wing is attached to a steel adapter clamped at its end instead of directly clamping the root of the wing.

In this paper, only the panels on the top are considered in the layup optimization. The previously optimized configurations in [42] are taken as starting points for the optimization presented here. In the previous optimization the stacking sequences of the skin panels, ribs and spars were fixed as [-45/45/90/0]s and only the layer thicknesses were optimized. Table 2 shows the starting layup information for this optimization.

Table 1 Material properties

Material properties	Values
Young's modulus in the fiber direction 1, E_{11}	140000 MPa
Young's modulus in the transverse direction 2, E_{22}	10000 MPa
Shear modulus G_{12}	5000 MPa
Poisson's ratio υ_{12}	0.3
Material density ρ	0.0016 $\mathrm{g/mm^3}$
Ultimate longitudinal tensile strength	1500 MPa
Ultimate longitudinal compressive strength	1200 MPa
Ultimate transverse tensile strength	50 MPa
Ultimate transverse compressive strength	250 MPa
Ultimate in-plane shear strength	70 MPa

Table 2 Starting layup and ply thicknesses (mm)

Top Panels		Panel 1	Panel 2	Panel 3	Panel 4	Panel 5	Panel 6
Skin	t(-45)	0.181	0.736	0.358	1.072	1.304	1.174
	t(45)	0.181	0.125	0.839	0.631	1.500	1.372
	t(90)	0.433	0.215	1.500	1.500	1.500	1.494
	t(0)	0.537	1.500	1.500	1.500	1.500	1.500
Web	t(-45)	0.159	0.282	0.364	0.265	0.308	1.208
	t(45)	0.188	0.282	0.503	0.221	0.308	1.395
	t(90)	0.354	0.125	0.963	0.964	0.125	2.242
	t(0)	0.817	1.500	2.000	2.000	0.125	2.499
Flange	t(-45)	0.280	0.593	1.500	1.500	1.467	1.173
	t(45)	0.280	0.641	1.500	1.500	1.467	1.173
	t(90)	0.559	0.236	1.500	1.500	1.545	1.448
	t(0)	1.500	1.500	2.000	2.000	2.500	2.500
Bottom Panels		Panel 7	Panel 8	Panel 9	Panel 10	Panel 11	Panel 12
Skin	t(-45)	0.13	0.13	0.13	0.13	0.13	0.13
	t(45)	0.13	0.13	0.13	0.13	0.13	0.13
	t(90)	0.54	0.88	0.13	0.13	0.13	0.13
	t(0)	0.13	0.14	0.25	0.32	0.55	0.7
Web	t(-45)	0.13	0.13	0.13	0.13	0.13	0.13
	t(45)	0.13	0.13	0.13	0.13	0.13	0.13
	t(90)	0.13	0.13	0.13	0.13	0.13	0.13
	t(0)	0.13	0.13	0.19	0.15	0.13	0.13
Flange	t(-45)	0.13	0.13	0.13	0.13	0.13	0.13
	t(45)	0.13	0.13	0.13	0.13	0.13	0.13
	t(90)	0.13	0.13	0.13	0.13	0.13	0.13
	t(0)	0.27	0.13	0.19	0.15	0.13	0.13

4.1 First stage optimization results

In the first stage of the optimization, four-node quadrilateral S4R shell elements [53] are used, being close to those used in the previous study of a wing box [42]. The numbers of elements used to mesh the geometry for the skin, webs and flanges of each component panel are 450, 75 and 75, respectively. Note that this mesh density results in missing a small number of local buckling modes which occur at the root of panel 1. The reason for this compromise in terms of the mesh is because the exact strip method assumes sinusoidal behaviour in the longitudimal direction and so cannot recognize these modes in the VICONOPT optimization. This is clearly a limitation of the VICONOPT MLO approach, and hence any replication of the optimization should take the same number of elements. The top panels are mainly subjected to compressive loading because they are on the top surface of the wing box. There are 21 design variables for each panel with the skin, web and flange having 7 variables each (i.e. $\xi_1^A, \xi_2^A, \xi_3^A, \xi_1^D, \xi_2^D, \xi_3^D, h$), hence a total of 126 design variables are specified in this optimization. Fig.9 (a) shows a total mass comparison for the top panels. As can be seen, the final mass of the first stage converges on a value of 49.1 kg. Compared with the optimized configuration in [42], a 4.9 kg reduction is achieved which represents a 9.1% saving over the previously optimized mass. It is observed that the design space is expanded by using lamination parameters as design variables. The mass change of each individual panel is shown in Fig.9 (b), where it can be seen that the majority of the mass saving of the whole structure is achieved in panels 2, 3 and 4 whose stacking sequences change significantly during the optimization. The mass reductions of panel 5 and 6 are relatively small, while the mass of panel 1 remains almost constant. As expected, the panel mass increases from the tip to the root due to the increase in bending moment along the wing. The panels on the right are heavier than the adjacent panels on the left due to the twisting effect resulting from the way the loads are applied. Table 3 shows the re-distributions of axial load and bending moment in each panel, obtained at the end of the multilevel optimization process based on the optimized structural configurations. Compared with the loading re-distributions of the optimized configurations in [42], it is observed that the newly optimized panels are able to carry approximately the same loads with reduced laminate thicknesses. The optimized lamination parameters and laminate thickness for each panel are listed in Table 4.

4.2 Second stage optimization results

In the second stage of the optimization, the lamination parameters obtained in the first stage are used as target values in the DLBB method. Due to manufacturing requirements, the ply thickness is chosen to be 0.125 mm in this case. For each panel, the number of plies after rounding up to the nearest larger integer number n is shown in the last column of Table 4. Although this will not result in the lightest weight solution, it will always ensure a safe solution. After the rounding process, for a wing constructed with the target lamination parameters, the buckling load factor for the first buckling mode, which is local to panel 1, is 1.15. The second buckling mode is a global buckling of the whole top surface for which the buckling load factor is 1.17.

Table 3 Re-distributions of axial load and bending moment after the multilevel optimization.

Panel no.		1	2	3	4	5	6
Axial load	Ref. 42	113.03	122.97	423.57	470.88	719.53	799.38
(kN)	This paper	110.79	121.80	422.22	462.88	710.24	804.46
Bending moment	Ref. 42	1.1963	5.4909	76.048	86.356	219.09	249.36
(kNm)	This paper	1.1492	2.6543	68.508	57.671	180.41	251.92

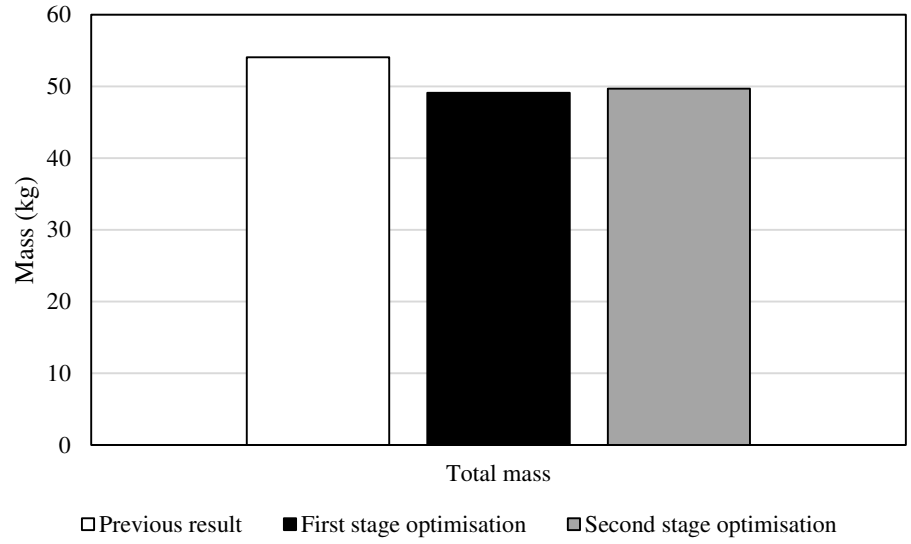

(a)

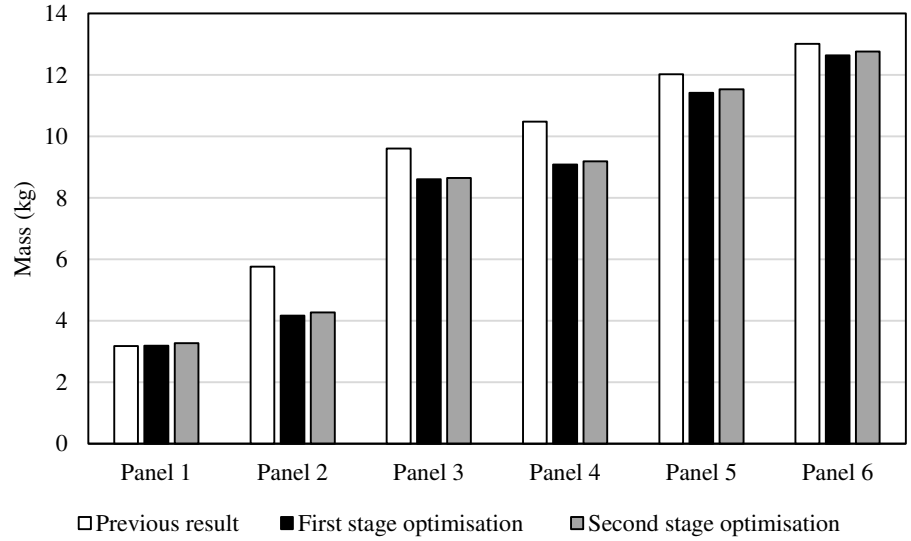

(b)

Fig. 9. (a) Total mass comparison of the top panels. (b) Mass comparisons of each individual panel.

Table 4 Optimization results of the first stage

Panel no.		ξ_1^A	ξ_2^A	ξ_3^A	ξ_1^D	ξ_2^D	ξ_3^D	h (mm)	n
1	Skin	0.0791	0.4552	-0.0006	-0.2559	-0.2245	-0.0959	2.674	22
	Web	0.3032	0.5392	0.0173	-0.1470	-0.0817	-0.0240	3.047	25
	Flange	0.3552	0.5678	-0.0035	-0.1069	-0.0247	-0.0612	5.257	43
2	Skin	0.266	0.1988	-0.0758	-0.0890	-0.1208	-0.4364	3.646	30
	Web	0.4225	0.4028	-0.0274	0.0512	-0.1266	-0.0589	3.598	29
	Flange	0.3024	0.0878	-0.0197	-0.0823	-0.5315	-0.1410	4.918	40
3	Skin	-0.0729	0.1781	-0.0208	-0.4108	-0.1073	0.0478	7.469	60
	Web	0.2158	0.4651	0.0019	-0.2970	0.0238	0.0132	7.101	57
	Flange	0.0527	0.0527	0	-0.1779	-0.5253	-0.0548	12.203	98
4	Skin	-0.0444	0.1639	-0.0359	-0.2338	-0.4526	-0.0274	8.156	66
	Web	0.2265	0.5485	-0.0131	-0.2851	0.2945	-0.0608	5.971	48
	Flange	0.0708	0.0709	0	-0.1286	-0.6492	-0.1735	11.273	91
5	Skin	0.0004	0.0338	0.0338	-0.1028	-0.7205	0.0384	11.027	89
	Web	0	-0.4225	0	-0.0180	-0.9529	-0.4905	1.645	14
	Flange	0.1368	0.1592	0	-0.1023	-0.6183	-0.2087	13.260	107
6	Skin	-0.0200	0.1013	0.0183	-0.1750	-0.4797	0.0114	10.761	87
	Web	0.0131	0.2141	-0.0011	-0.2058	-0.4636	-0.0792	14.261	115
	Flange	0.1537	0.2174	-0.0221	-0.1471	-0.4700	-0.1508	12.342	99

4.2.1 Layup design without blending constraint

In order to validate the DLBB method, in this section the stacking sequences are optimized using the LBB method presented in Section 2.2, without imposing the blending constraint. Table 5 shows the optimized stacking sequences considering only the four layup design constraints. Compared with the previous results in [42], the stacking sequences obtained here are more realistic and have more anisotropy. The lamination parameters related to the optimized stacking sequences together with their Γ are listed in Table 6. As can be seen, the values of Γ are small, meaning the lamination parameters of the obtained stacking sequences are good matches for the target lamination parameters. The thicker laminates have relatively lower values of Γ, because they have a larger number of plies making their stacking sequences easier to match with the targets. After the stacking sequences are obtained, the optimized configuration is checked for buckling with ABAQUS. Results show that the local and global buckling load factors (i.e. the first and second buckling modes) are 1.09 and 1.15, respectively. Comparison of these buckling load factors obtained using the stacking sequences with those obtained using the target lamination parameters directly, shows that there is only a small decrease of buckling performance caused by the mismatch between the target lamination parameters and the actual stacking sequences. Therefore, the stacking sequences obtained separately based on the four layup design constraints in the second stage of the optimization have lamination parameters close to the optimized values obtained in the first stage.

Table 5 Stacking sequences of top panels without blending constraint

Panel no.		Stacking sequences
1	Skin	[45/-45/90$_2$/-45/0$_4$/45/90]$_S$
	Web	[45/-45/90$_2$/-45/0$_2$/45/0$_4$/45]$_{MS}$
	Flange	[45/-45$_2$/90$_4$/45/0$_3$/-45/0$_4$/45/0$_4$/-45]$_{MS}$
2	Skin	[45/-45/90$_2$/-45$_2$/0$_2$/-45/0$_4$/45/90]$_S$
	Web	[45/-45/90$_2$/-45/0$_4$/45/0$_4$/-45]$_{MS}$
	Flange	[45/-45$_4$/90/45$_2$/90/45/0$_3$/-45/0$_3$/45/0$_2$]$_S$
3	Skin	[45/-45/90/45$_2$/90/-45/90$_2$/45/90/-45/90/(-45/90$_2$) $_2$/-45/0$_2$/45/0$_4$/45/0$_2$]$_S$
	Web	[45/-45$_2$/90$_3$/(45/90) $_2$/-45/90$_2$/45/0$_4$/-45/0$_4$/45/0$_4$/-45]$_{MS}$
	Flange	[45/-45$_4$/90/45$_4$/90/-45$_3$/90/45$_2$/90/-45$_3$/90/45/90$_3$/45/0$_2$/45/90$_2$/45/0$_4$/ (-45/0$_4$) $_2$/45/90]$_S$
4	Skin	[45/-45$_4$/90/45$_4$/90/-45/90/45/90$_2$/-45/90$_4$/45/0$_4$/-45/0$_4$/-45/90]$_S$
	Web	[45/-45/90$_4$/-45/90$_2$/-45/(0$_4$/45) $_2$/0$_3$/-45]$_S$
	Flange	[45/-45$_4$/90/-45$_4$/90/45$_4$/90/45$_3$/90/-45/90$_4$/(-45/0$_4$) $_2$/45/0$_4$/45/90$_2$/45/0/0]$_{MS}$
5	Skin	[45/-45$_4$/90/45$_4$/90/-45/90/45$_4$/0/-45$_3$/0/-45/0$_2$/(45/90$_4$) $_2$/45/0$_3$/-45/0$_4$/-45]$_{MS}$
	Web	[45/-45$_3$/90/45/0]$_S$
	Flange	[45/-45$_4$/90/-45$_4$/90/-45$_2$/90/45$_4$/90/45$_2$/90$_3$/-45/0/45(0$_4$/45)$_2$/90$_4$/-45/ (0$_4$/45) $_2$/0/0]$_{MS}$
6	Skin	[45/-45$_4$/90/45$_4$/90/45$_3$/90/-45$_3$/90/-45/90$_4$/-45/0$_3$/45/0$_4$/45/90$_4$/-45/0$_4$/45]$_{MS}$
	Web	[45/-45$_4$/90/45$_4$/90/-45$_4$/90/45$_3$/90/-45$_3$/90$_2$/45/90$_4$/-45/90$_4$/45/0$_4$/-45/ (0$_4$/45) $_3$/90/90]$_{MS}$
	Flange	[45/-45$_4$/90/-45$_3$/90/45$_4$/90/45/90/-45$_3$/90/45$_2$/0/-45/90$_4$/(45/0$_4$)$_3$/-45/0$_4$/-45]$_{MS}$

Table 6 Lamination parameters of the optimized stacking sequences without blending constraint

Panel no.		ξ_1^A	ξ_2^A	ξ_3^A	ξ_1^D	ξ_2^D	ξ_3^D	Γ
1	Skin	0.0909	0.2727	0	-0.1345	-0.1059	-0.0451	0.4857
	Web	0.3200	0.2800	0.0400	-0.1009	-0.0886	-0.0245	0.3523
	Flange	0.3256	0.3953	-0.0233	-0.1206	0.0802	-0.0601	0.3415
2	Skin	0.2000	0.2000	-0.1333	-0.0809	-0.1342	-0.1890	0.3936
	Web	0.4138	0.3793	-0.0345	-0.0044	0.0349	-0.0473	0.2680
	Flange	0.3000	0	0	-0.0217	-0.5295	-0.1380	0.1755
3	Skin	-0.0667	0.2000	0	-0.3867	-0.1062	0.0482	0.0745
	Web	0.1754	0.3333	0.0175	-0.2834	0.0286	0.0115	0.2079
	Flange	0.0612	0.0204	0	-0.1707	-0.4474	-0.0544	0.1264
4	Skin	-0.0606	0.0909	-0.0303	-0.2273	-0.4123	-0.0259	0.1431
	Web	0.2083	0.4167	-0.0417	-0.2852	0.2681	-0.0782	0.2225
	Flange	0.0769	0.0330	0	-0.1390	-0.4555	-0.1711	0.2506
5	Skin	0	-0.0112	0.0337	-0.1039	-0.4819	0.0349	0.2887
	Web	0	-0.4286	-0.1429	-0.0525	-0.8834	-0.1603	0.5831
	Flange	0.1402	0.1028	0	-0.1085	-0.3778	-0.2093	0.3071
6	Skin	-0.0230	0.0575	0.0115	-0.1660	-0.4450	0.0141	0.1001
	Web	0.0087	0.0957	0	-0.2120	-0.3976	-0.0814	0.1983
	Flange	0.1616	0.0505	-0.0303	-0.1465	-0.4302	-0.1498	0.2244

Table 7 Stacking sequences of skins with blending constraint.

Panel no.	Stacking sequences
5	[45/−45/−45$_2$/−45/90/45$_2$/45/45/90/−45/−45/90/45/45$_2$/**45**/90/−45/90/45/90/−45/0$_2$/0/−45/90$_3$/90/45/0$_2$/0$_2$/−45/0$_2$/0$_2$/45/90/90]$_{MS}$
6	[45/−45/−45$_2$/−**45**/90/45$_2$/45/**45**/90/−45/−**45**/90/45/**45$_2$**/90/−45/90/**45**/90/−45/0$_2$/**0**/−45/90$_3$/**90**/45/0$_2$/**0$_2$**/−45/0$_2$/0$_2$/45/90/**90**]$_{MS}$
4	[45/−45/−**45$_2$**/90/45$_2$/**45**/90/−45/90/45/90/−45/90$_2$/−45/0$_2$/−45/90$_3$/45/0$_2$/−45/0$_2$/0$_2$/45/90]$_S$
3	[45/−45/**90/45$_2$/90**/−45/90/**45**/90/−**45**/90/**90**/−45/0$_2$/−**45/90$_3$/45**/0$_2$/−45/0$_2$/**0$_2$**/45/**90**]$_S$
2	[45/−45/−**45**/90$_3$/−45/0$_4$/−**45/0$_2$**/45]$_S$
1	[45/−45/90$_3$/−45/0$_4$/45]$_S$

Table 8 Stacking sequences of the left and right hand side flanges with blending constraint.

Panel no.	Stacking sequences
	left hand side flanges
5	[45/−45/−45$_3$/90/−45/−45$_2$/−**45**/90/45/45$_2$/90/−45/−45/90/45$_3$/90$_2$/45/90/−45/0$_4$/45/0$_2$/**0**/−45/0$_2$/45/0$_2$/**0$_2$**/45/90$_4$/−45/0$_3$/45/0/**0**]$_{MS}$
3	[45/−45/−**45$_3$**/90/−45/−**45$_2$**/90/45/**45$_2$**/90/−45/−**45/90/45$_3$/90$_2$/45/90**/−**45**/0$_4$/45/0$_2$/−**45**/0$_2$/**45/0$_2$/45/90$_4$**/−45/0$_3$/45/**0**]$_S$
1	[45/−45/90/−45/90/45/90/−45/0$_4$/45/0$_4$/−45/0$_3$/45]$_{MS}$
	right hand side flanges
6	[45/−45$_4$/90/−45$_4$/90/45$_2$/45$_2$/90/45/45/90/−**45**/90$_2$/−45/0/45/0/**0$_3$**/−45/0$_4$/45/90$_4$/−45/0$_2$/0$_2$/45/0$_4$/45]$_{MS}$
4	[45/−45$_4$/90/−**45$_4$/90**/45$_2$/**45$_2$**/90/45/**45/90$_3$**/−**45**/0/**45**/0/−45/0$_4$/45/**90$_4$**/−**45**/0$_2$/**0$_2$/45/0$_4$/45**]$_{MS}$
2	[45/−45$_4$/90/45$_2$/90/45/0$_2$/−45/0$_4$/45/0$_2$]$_S$

Table 9 Stacking sequences of the left and right hand side webs with blending constraint.

Panel no.	Stacking sequences
	left hand side webs
3	[45/−45/−**45**/90/**45**/90/**90/45/90$_3$**/−45/0$_3$/**0/45/0$_2$**/−45/90/−**45/0$_4$**/45/0/0]$_{MS}$
1	[45/−45/**90$_2$**/−45/**0$_3$**/−45/90/45/0/**0**]$_{MS}$
5	[45/−45$_3$/90/45/0]$_S$
	right hand side webs
6	[45/−45/−**45$_3$**/90/−**45**/90/**45$_3$**/90/**45**/90/−45/90/**90**/−45/**90$_3$**/−**45**/0$_4$/45/**90/45**/0/**45/90$_3$**/−**45**/0$_3$/**0**/45/**90$_2$**/−**45**/0$_3$/−45/90/**90**/**(45/0$_2$)$_2$/0$_2$**/−**45**]$_{MS}$
4	[45/−45/90$_2$/**90$_2$**/−45/**90**/−**45**/0$_4$/45/0$_4$/**45/0$_3$**/−45/**90**]$_S$
2	[45/−45/90$_2$/−45/0$_4$/45/0$_4$/−45]$_{MS}$

Table 10 Lamination parameters of the blended stacking sequences of skins

Panel no.	ξ_1^A	ξ_2^A	ξ_3^A	ξ_1^D	ξ_2^D	ξ_3^D	Γ
5	−0.0112	0.0112	0.0449	−0.1595	−0.4716	0.0269	0.3624
6	−0.0115	0.0345	0.0230	−0.1632	−0.4493	−0.0011	0.1346
4	−0.0606	0.0909	−0.0303	−0.2286	−0.3262	−0.0419	0.2410
3	−0.0667	0.2000	0	−0.2981	−0.1156	0.0596	0.1817
2	0.2000	0.2000	−0.1333	−0.1556	−0.1271	−0.1890	0.4450
1	0.0909	0.2727	0	−0.2923	−0.0428	−0.0225	0.4863

Table 11 Lamination parameters of the blended stacking sequences of left and right hand side flanges.

Panel no.	ξ_1^A	ξ_2^A	ξ_3^A	ξ_1^D	ξ_2^D	ξ_3^D	Γ
left hand side flanges							
5	0.1215	0.0654	−0.0187	−0.0933	−0.3958	−0.1832	0.3848
3	0.0612	0.0204	0	−0.1245	−0.4075	−0.1558	0.3131
1	0.3721	0.3023	−0.0233	−0.0460	−0.0352	−0.0477	0.3870
right hand side flanges							
6	0.1414	0.0909	−0.0303	−0.0898	−0.4050	−0.1720	0.2904
4	0.0879	0.0549	−0.0110	−0.1250	−0.4365	−0.1695	0.2644
2	0.3000	0	0	−0.0270	−0.5400	−0.1432	0.1760

Table 12 Lamination parameters of the blended stacking sequences of left and right hand side webs.

Panel no.	ξ_1^A	ξ_2^A	ξ_3^A	ξ_1^D	ξ_2^D	ξ_3^D	Γ
left hand side webs							
3	0.1579	0.2982	0	−0.2116	0.0219	0.0162	0.3170
1	0.1200	0.2000	−0.0800	−0.1212	−0.0734	−0.0815	0.7114
5	0	−0.4286	−0.1429	−0.0525	−0.8834	−0.1603	0.5831
right hand side webs							
6	0.0174	0.2174	−0.0087	−0.2044	−0.1122	−0.0785	0.3687
4	0.2083	0.4167	−0.0417	−0.1945	0.2412	−0.0786	0.3403
2	0.4138	0.3793	−0.0345	−0.0044	0.0349	−0.0473	0.2680

Table 13 Summary of the comparisons between LBB with GA in [1]

Single laminate	GAs (averaged for 10 runs)	LBB	
	Γ after 300s	Γ after 300s	Time to find this Γ
Example 1	0.1053	0.0806	4.77s
Example 2	0.0948	0.0892	3.76s

Table 14 Change of Γ during the DLBB optimization

Blended laminates	DLBB				
	Initial Γ	Γ after 300s	Γ after 1000s	Γ after 3000s	Γ after 10000s
Skin	6.4431	2.4289	2.1264	2.0602	1.8508
Right flange	3.1800	0.8355	0.7794	0.7646	0.7308
Left flange	3.2350	1.0966	1.0954	1.0898	1.0849
Right web	3.8704	1.0982	1.0763	1.0671	0.9770
Left web	3.8335	1.8325	1.7140	1.6126	1.6115

4.2.2 Layup design with blending constraint

Tables 7-9 show the optimized stacking sequences obtained using the DLBB method, which satisfy the four layup design constraints and also the blending constraint. There are five separate blending problems including the skins of all of the top panels, the webs of the left hand side panels (i.e. panels 1, 3 and 5) and the right hand side panels (i.e. panels 2, 4 and 6) respectively, and the flanges of the left and right hand panels respectively, the dropped plies are shown bold in Tables 7-9. In this paper, no

constraints are applied between the skin, webs and flanges, which are treated as independent laminates in the second stage. The related lamination parameters and the Γ are summarised in Tables 10-12. As can be seen, the values of Γ in Tables 10-12 are higher than those in Table 6 because the blending constraint narrows the design space and hence reduces the level of match between the target and obtained lamination parameters. For the five blending problems, with the exception of the webs on the left hand side, the increase in the value of Γ for each laminate is acceptable. However, as the numbers of plies in the webs on the left hand side are small (which will not be the case in a more realistic aircraft wing design), the blending constraint causes an additional mismatch between the target and obtained lamination parameter for the web in panel 1 equal to 0.3591, with the majority of the mismatch being on $\xi_{1,2}^{A}$. Since the stiffness of each panel is mainly provided by the skin and flanges, this mismatch only has a small effect on the load-carrying capability of the wing. When the obtained stacking sequences are checked by FEA using ABAQUS, results show that the local and global buckling load factors (corresponding to the first and second buckling modes) decrease to 1.08 and 1.14, respectively. It is observed that there is only a slight decrease in the buckling performance when adding the blending constraint, and that the optimized configuration still satisfies the buckling constraint. The performance of the DLBB method in optimizing blended stacking sequences to match the target lamination parameters from the first stage optimization is illustrated. Note that, due to the rounding process at the start of the second stage, the weight of the final optimized wing box is increased slightly to 49.7 kg as shown in Fig. 9. Compared with the results in [42], the stacking sequences of the optimized wing box presented here are more manufacturable, and the weight of the structure is reduced by 8.0%, which will lead to reductions in the material cost and fuel consumption of the aircraft.

In [1] the logic-based method is proven to be more efficient than a stochastic search based on GAs. A summary of these comparisons is shown in Table 13. In this paper, the efficiency of the DLBB method is illustrated in Table 14 by showing the changes in Γ for the five blending problems during the second stage optimization. As can be seen, the biggest reductions in the values of Γ are achieved in the first 300s after which the level of reduction is much smaller, especially for the blending problems comprising only a small number of plies. Good results can therefore be obtained efficiently at early stages of the application of the DLBB method, and for practical design the optimization can be stopped once an acceptable result is found (e.g. when Γ is lower than a specific value).

5. Conclusions

This paper presents a two-stage layup optimization methodology using lamination parameters for the weight minimization of blended composite structures under buckling, lamination parameter, layup design and blending constraints. In the first stage, stacking sequences are replaced by lamination parameters and laminate thicknesses as design variables to permit the design of more manufacturable layups in the multilevel optimization software VICONOPT MLO. The optimized lamination parameters derived are then used as targets in the second stage in which, instead of the more commonly used heuristic methods for performing a stochastic search, a new logic-based DLBB method combining a dummy layerwise technique with the branch and bound method is proposed to search the stacking sequences which satisfy the blending and layup design constraints to match the targets. The effectiveness of the two-stage method for optimizing blended laminates is demonstrated by a benchmark problem based on an aircraft wing box. Comparison of the results obtained using the new method with the results in [42] shows a further weight reduction of 8.0% can be achieved over the previously determined wing weight even when more constraints are added, making the optimized structure more manufacturable and improving its performance. Nevertheless, in the current study, only

the four ply angles 0°, 90°, +45° and -45° are considered in the optimization. As a line of future research, the DLBB method could be extended by adding more permissible fiber orientations with the consideration of more layup design rules as well as expanding the complexity of the objective function to improve the efficiency.

Acknowledgement

The first author is grateful for financial support from the China Scholarship Council.

References

[1] X. Liu, C.A. Featherston, D. Kennedy, Two-level layup optimization of composite laminate using lamination parameters, Compos. Struct. 211 (2019) 337–350. https://doi.org/10.1016/j.compstruct.2018.12.054.

[2] B.P. Kristinsdottir, Z.B. Zabinsky, M.E. Tuttle, S. Neogi, Optimal design of large composite panels with varying loads, Compos. Struct. 51 (2001) 93–102. https://doi.org/10.1016/S0263-8223(00)00128-8.

[3] G. Soremekun, Z. Gürdal, C. Kassapoglou, D. Toni, Stacking sequence blending of multiple composite laminates using genetic algorithms, Compos. Struct. 56 (2002) 53–62. https://doi.org/10.1016/S0263-8223(01)00185-4.

[4] D.B. Adams, L.T. Watson, Z. Gürdal, C.M. Anderson-Cook, Genetic algorithm optimization and blending of composite laminates by locally reducing laminate thickness, Adv. Eng. Softw. 35 (2004) 35–43. https://doi.org/10.1016/j.advengsoft.2003.09.001.

[5] D.B. Adams, L.T. Watson, Z. Gürdal, Optimization and Blending of Composite Laminates Using Genetic Algorithms with Migration Optimization and Blending of Composite Laminates, Mech. Adv. Mater. Struct. 10 (2003) 37–41. https://doi.org/10.1080/15376490306741.

[6] D.B. Adams, L.T. Watson, O. Seresta, Z. Gürdal, Global/local iteration for blended composite laminate panel structure optimization subproblems, Mech. Adv. Mater. Struct. 14 (2007) 139–150. https://doi.org/10.1080/15376490600719212.

[7] F.X. Irisarri, A. Lasseigne, F.H. Leroy, R. Le Riche, Optimal design of laminated composite structures with ply drops using stacking sequence tables, Compos. Struct. 107 (2014) 559–569. https://doi.org/10.1016/j.compstruct.2013.08.030.

[8] H.T. Fan, H. Wang, X.H. Chen, An optimization method for composite structures with ply-drops, Compos. Struct. 136 (2016) 650–661. https://doi.org/10.1016/j.compstruct.2015.11.003.

[9] H. An, S. Chen, H. Huang, Stacking sequence optimization and blending design of laminated composite structures, Struct. Multidiscip. Optim. 59 (2019). https://doi.org/10.1007/s00158-018-2158-1.

[10] B. Liu, R. Haftka, Composite wing structural design optimization with continuity constraints, in: 19th AIAA Appl. Aerodyn. Conf., American Institute of Aeronautics and Astronautics, Anaheim,CA, 2001. https://doi.org/10.2514/6.2001-1205.

[11] O. Seresta, Z. Gürdal, D.B. Adams, L.T. Watson, Optimal design of composite wing structures with blended laminates, Compos. Part B Eng. 38 (2007) 469–480. https://doi.org/10.1016/j.compositesb.2006.08.005.

[12] Z. Jing, X. Fan, Q. Sun, Global shared-layer blending method for stacking sequence optimization design and blending of composite structures, Compos. Part B Eng. 69 (2015)

181–190. https://doi.org/10.1016/j.compositesb.2014.09.039.

[13] Z. Jing, J. Chen, Q. Sun, Constrained-manufacturable stacking sequence design optimization using an improved global shared-layer blending method and its 98-line Matlab code, Struct. Multidiscip. Optim. 59 (2019) 539–575. https://doi.org/10.1007/s00158-018-2083-3.

[14] M. Miki, Y. Sugiyama, Optimum design of laminated composites plates using lamination parameters, AIAA J. 31 (1993) 921–922. https://doi.org/10.2514/3.49033.

[15] H. Fukunaga, H. Sekine, M. Sato, A. Iino, Buckling design of symmetrically laminated plates using lamination parameters, Comput. Struct. 57 (1995) 643–649. https://doi.org/10.1016/0045-7949(95)00050-Q.

[16] K. Yamazaki, Two-level optimization technique of composite laminate panels by genetic algorithms, Collect. Tech. Pap. - AIAA/ASME/ASCE/AHS/ASC Struct. Struct. Dyn. Mater. Conf. 3 (1996) 1882–1887. https://doi.org/doi:10.2514/6.1996-1539.

[17] A. Todoroki, Y. Terada, Improved Fractal Branch and Bound Method for Stacking-Sequence Optimizations of Laminates, AIAA J. 42 (2004) 141–148. https://doi.org/10.2514/1.9038.

[18] M. Kameyama, H. Fukunaga, Optimum design of composite plate wings for aeroelastic characteristics using lamination parameters, Comput. Struct. 85 (2007) 213–224. https://doi.org/10.1016/j.compstruc.2006.08.051.

[19] J.E. Herencia, P.M. Weaver, M.I. Friswell, Initial sizing optimisation of anisotropic composite panels with T-shaped stiffeners, Thin-Walled Struct. 46 (2008) 399–412. https://doi.org/10.1016/j.tws.2007.09.003.

[20] M.W. Bloomfield, J.E. Herencia, P.M. Weaver, Enhanced two-level optimization of anisotropic laminated composite plates with strength and buckling constraints, Thin-Walled Struct. 47 (2009) 1161–1167. https://doi.org/10.1016/j.tws.2009.04.008.

[21] F.-X. Irisarri, M.M. Abdalla, Z. Gürdal, Improved Shepard's Method for the Optimization of Composite Structures, AIAA J. 49 (2012) 2726–2736. https://doi.org/10.2514/1.j051109.

[22] D. Liu, V. V. Toropov, A lamination parameter-based strategy for solving an integer-continuous problem arising in composite optimization, Comput. Struct. 128 (2013) 170–174. https://doi.org/10.1016/j.compstruc.2013.06.003.

[23] T.A. Dutra, S.F.M. Almeida, Composite plate stiffness multicriteria optimization using lamination parameters, Compos. Struct. 133 (2015) 166–177. https://doi.org/10.1016/j.compstruct.2015.07.029.

[24] S.T. IJsselmuiden, M.M. Abdalla, O. Seresta, Z. Gürdal, Multi-step blended stacking sequence design of panel assemblies with buckling constraints, Compos. Part B Eng. 40 (2009) 329–336. https://doi.org/10.1016/j.compositesb.2008.12.002.

[25] D. Liu, V. V. Toropov, D.C. Barton, O.M. Querin, Weight and mechanical performance optimization of blended composite wing panels using lamination parameters, Struct. Multidiscip. Optim. 52 (2015) 549–562. https://doi.org/10.1007/s00158-015-1244-x.

[26] T. Macquart, M.T. Bordogna, P. Lancelot, R. De Breuker, Derivation and application of blending constraints in lamination parameter space for composite optimisation, Compos. Struct. 135 (2016). https://doi.org/10.1016/j.compstruct.2015.09.016.

[27] T. Macquart, N. Werter, R. De Breuker, Aeroelastic Design of Blended Composite Structures Using Lamination Parameters, J. Aircr. 54 (2017) 561–571. https://doi.org/10.2514/1.C033859.

[28] M.T. Bordogna, T. Macquart, D. Bettebghor, R. De Breuker, Aeroelastic optimization of variable stifiness composite wing with blending constraints, 17th AIAA/ISSMO Multidiscip.

Anal. Optim. Conf. (2016). https://doi.org/10.2514/6.2016-4122.

[29] M.T. Bordogna, P. Lancelot, D. Bettebghor, R. De Breuker, Static and dynamic aeroelastic tailoring with composite blending and manoeuvre load alleviation, Struct. Multidiscip. Optim. (2020). https://doi.org/10.1007/s00158-019-02446-w.

[30] Y.M. Meddaikar, F.X. Irisarri, M.M. Abdalla, Laminate optimization of blended composite structures using a modified Shepard's method and stacking sequence tables, Struct. Multidiscip. Optim. 55 (2017) 535–546. https://doi.org/10.1007/s00158-016-1508-0.

[31] E. Panettieri, M. Montemurro, C. Anita, Blending constraints for composite laminates in polar parameters space.pdf, Compos. Part B Eng. 168 (2019) 448–457. https://doi.org/10.1016/j.compositesb.2019.03.040.

[32] S. Zein, P. Basso, S. Grihon, A constraint satisfaction programming approach for computing manufacturable stacking sequences, Comput. Struct. 136 (2014) 56–63. https://doi.org/10.1016/j.compstruc.2014.01.016.

[33] S. Zein, V. Madhavan, D. Dumas, L. Ravier, I. Yague, From stacking sequences to ply layouts: An algorithm to design manufacturable composite structures, Compos. Struct. 141 (2016) 32–38. https://doi.org/10.1016/j.compstruct.2016.01.027.

[34] J. Sanz-Corretge, A constraint satisfaction problem algorithm for large-scale multi-panel composite structures, Struct. Multidiscip. Optim. 60 (2019) 2035–2051. https://doi.org/10.1007/s00158-019-02309-4.

[35] S.N. Sørensen, R. Sørensen, E. Lund, DMTO - A method for Discrete Material and Thickness Optimization of laminated composite structures, Struct. Multidiscip. Optim. 50 (2014) 25–47. https://doi.org/10.1007/s00158-014-1047-5.

[36] J.H. Sjølund, D. Peeters, E. Lund, A new thickness parameterization for Discrete Material and Thickness Optimization, Struct. Multidiscip. Optim. 58 (2018) 1885–1897. https://doi.org/10.1007/s00158-018-2093-1.

[37] R. Butler, F.W. Williams, Optimum design using VICONOPT, a buckling and strength constraint program for prismatic assemblies of anisotropic plates, Comput. Struct. 43 (1992) 699–708. https://doi.org/10.1016/0045-7949(92)90511-W.

[38] D. Kennedy, C.A. Featherston, Exact strip analysis and optimum design of aerospace structures, Aeronaut. J. 114 (2010) 505–512. https://doi.org/10.1017/S0001924000003997.

[39] D. Kennedy, B. Park, M.D. Unsworth, Towards Global Layup Optimization of Composite Panels with Initial Buckling Constraints, in: Proceeding 8th ASMO UK/ISSMO Conf., London, 2010: pp. 221–231.

[40] W.H. Wittrick, F.W. Williams, A general algorithm for computing natural frequencies of elastic structures, Q. J. Mech. Appl. Math. 24 (1971) 263–284. https://doi.org/10.1093/qjmam/24.3.263.

[41] W.H. Wittrick, F.W. Williams, An algorithm for computing critical buckling loads of elastic structures, J. Struct. Mech. 1 (1973) 497–518. https://doi.org/10.1080/03601217308905354.

[42] M. Fischer, D. Kennedy, C. a. Featherston, Multilevel framework for optimization of lightweight structures, Proc. Inst. Mech. Eng. Part G J. Aerosp. Eng. 226 (2012) 380–394. https://doi.org/10.1177/0954410011411637.

[43] S. Qu, D. Kennedy, C.A. Featherston, A multilevel framework for optimization of an aircraft wing incorporating postbuckling effects, Proc. Inst. Mech. Eng. Part G J. Aerosp. Eng. 226 (2011) 830–845. https://doi.org/10.1177/0954410011415158.

[44] W.H. Wittrick, F.W. Williams, Buckling and vibration of anisotropic or isotropic plate

assemblies under combined loadings, Int. J. Mech. Sci. 16 (1974) 209–239. https://doi.org/10.1016/0020-7403(74)90069-1.

[45] M.S. Anderson, F.W. Williams, C.J. Wright, Buckling and vibration of any prismatic assembly of shear and compression loaded anisotropic plates with an arbitrary supporting structure, Int. J. Mech. Sci. 25 (1983) 585–596. https://doi.org/10.1016/0020-7403(83)90050-4.

[46] G.N. Vanderplaats, F. Moses, Structural optimization by methods of feasible directions, Comput. Struct. 3 (1973) 739–755. https://doi.org/10.1016/0045-7949(73)90055-2.

[47] M.C.Y. Niu, Laminate Design Practices, Compos. Airframe Struct. (1992) 383–452. http://www.aerostudents.com/master/advancedDesignAndOptimizationOfCompositeStructures.php.

[48] R.M. Jones, Mechanics Of Composite Materials, second edi, Taylor and Francis, New York, 1999.

[49] C.G. Diaconu, H. Sekine, Layup optimization for buckling of laminated composite shells with restricted layer angles, AIAA J. 42 (2004) 2153–2163. https://doi.org/https://doi.org/10.2514/1.931.

[50] C.G. Diaconu, M. Sato, H. Sekine, Feasible Region in General Design Space of Lamination Parameters for Laminated Composites, AIAA J. 40 (2002) 559–565. https://doi.org/10.2514/2.1683.

[51] M.W. Bloomfield, C.G. Diaconu, P.M. Weaver, On feasible regions of lamination parameters for lay-up optimization of laminated composites, Proc. R. Soc. A Math. Phys. Eng. Sci. 465 (2009) 1123–1143. https://doi.org/10.1098/rspa.2008.0380.

[52] Dassault Systèmes, ABAQUS, version 6.12, (2013).